

# Structural stability of concrete wind turbines and solar chimney towers exposed to dynamic wind action

Reinhard Harte<sup>a,\*</sup>, Gideon P.A.G. Van Zijl<sup>b</sup>

<sup>a</sup>*Civil Engineering Department, Bergische Universität Wuppertal, Pauluskirchstr. 7, 42285 Wuppertal, Germany*

<sup>b</sup>*Division for Structural Engineering, University of Stellenbosch, Private Bag XI, Matieland 7602, South Africa*

Available online 29 March 2007

---

## Abstract

Apart from burning classical fossil resources or generating nuclear power, alternatives have been developed, like the classical ways to capture energy from wind, water and sun, or the innovative solar chimney concept.

The paper presents some structural aspects of classical wind energy turbines, like their high-cycle dynamic loading and reaction as well as their fatigue behaviour. Actual research results concerning pre-stressed concrete tower constructions for wind turbines will be focused on. For the solar chimney concept the structural challenges concerning wind action, eigenfrequencies, stiffening and shape optimization with special focus on the inlet guide vanes will be discussed. Both classical wind turbines and the innovative solar chimney concept may successfully contribute to the future energy supply in Southern Africa.

© 2007 Elsevier Ltd. All rights reserved.

*Keywords:* Wind turbines; High-cycle excitation; Fatigue; Damage; Solar chimney; Wind-structure interaction; Inlet guide vanes

---

---

\*Corresponding author. Tel.: +49 202 4394080; fax: +49 202 4394078.

E-mail addresses: [harte@uni-wuppertal.de](mailto:harte@uni-wuppertal.de) (R. Harte), [gvanzijl@sun.ac.za](mailto:gvanzijl@sun.ac.za) (G.P.A.G. Van Zijl).

### 1. Classical wind turbines

#### 1.1. Development of wind energy

The development of wind-energy can be demonstrated by the accumulated installed capacity in Figs. 1 and 2: Europe provides 72.5% of wind energy capacity, North America 15.0%, Asia 7.9%, whereas the large continent Africa contributes insignificantly. So, this large continent still offers the opportunity to serve the economic growth not by environment-polluting fossil and nuclear energy plants, but by renewable energy sources, such as water, wind and sun. Here, approved technologies like wind turbines as well as innovative future technologies like solar chimneys may contribute significantly.

#### 1.2. Structural challenges

Different structural alternatives exist for the mast of a wind turbine. First, steel lattice-towers have been used, but they consist of a large number of different elements, with the disadvantages of time-consuming mounting and durability concerns. The numerous connections are exposed to corrosion, and the weak diagonals are often sensitive to wind excitation. Later cylindrical steel tube towers have been preferred in Germany, as the rapid mounting by the assemblage of 2 or 3 prefabricated tube segments with flanges and bolts definitely minimizes the erection time on site. This, as well as the elegant design made steel tube towers the most popular in Germany (Fig. 3).

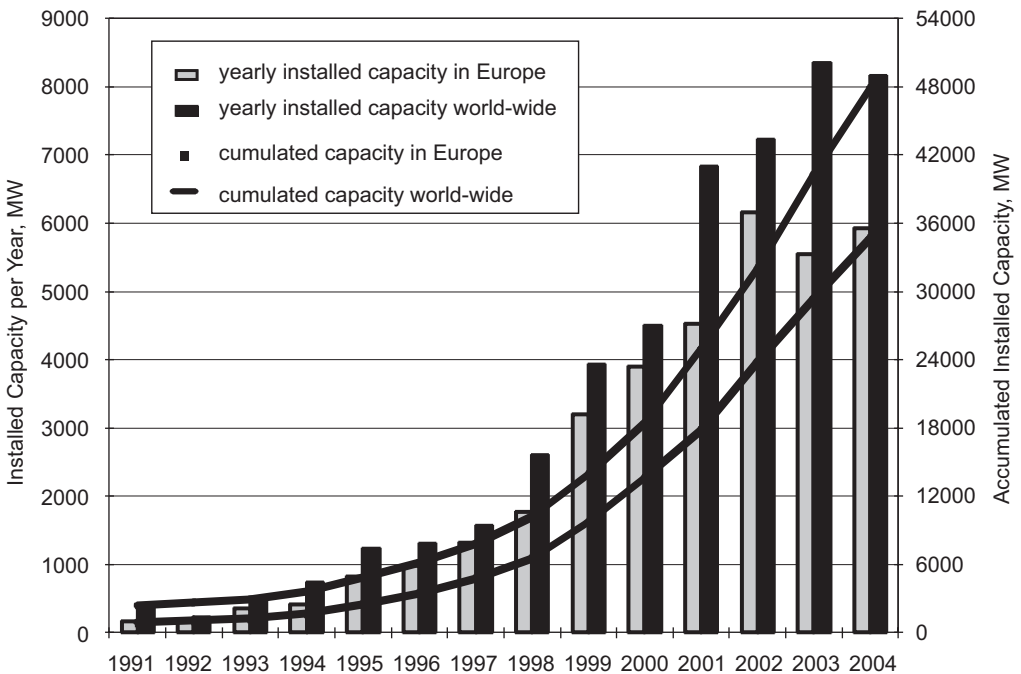


Fig. 1. Development of the wind energy use (DEWI, 2005).

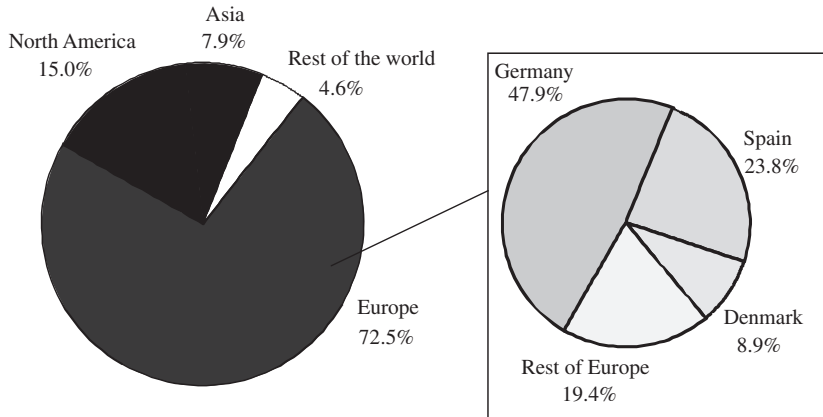


Fig. 2. Wind energy use world-wide (DEWI, 2005).

Increasing turbine capacities demand larger rotor diameters and tower heights. In case of exceeding 85 m height, steel tube towers are no longer able to balance the vibration excitation. Then concrete towers are more appropriate. They can be built with sliding or climbing formworks, both techniques which are well established and approved in chimney and cooling tower industry. Pre-stressing is necessary to meet the wind tensile forces. The stiffer concrete structure allows larger dimensions and thus optimized turbine capacities and energy output. For European countries with their lack of suitable space this is a matter of necessity, whereas for countries and continents with smaller populations but large space like Australia or Africa smaller units in large-sized wind-parks, or single units for smallholders may be more suitable. In this case steel tube towers still might be the appropriate alternative.

### 1.3. High-cycle excitation

Civil engineering structures in general are designed with a defined safety margin against resonant excitation. The dynamic response will be estimated by the quasi-static stress state multiplied by a corresponding amplification factor, depending on the eigenfrequency of the structure. However, in case of fracture and cracking of concrete the eigenfrequencies may change drastically, thus influencing the dynamic amplification and the ultimate limit capacity of the structure as well.

For wind turbines the eigenfrequencies of the overall structure with foundation, tower, machine and rotor blades have to be evaluated and compared with the external excitations by

- the wind turbulence
- the periodic excitation due to the turbine's rotation: the turbine frequency  $f_{1p}$
- the periodic excitation due to the rotor blades' interaction with the tower axis: the rotor blade frequency  $f_{3p}$  (in case of a 3-rotor-blade-turbine).

Then the design criterion is to keep the eigenfrequencies sufficiently far away from the periodic excitation, considering a  $\pm 10\%$  tolerance (Fig. 4).



Fig. 3. Steel tube towers (Enercon).

For small turbines it is easy to design the towers stiff enough in order to shift the eigenfrequencies beyond the excitation—a so-called “stiff-stiff” construction. Today’s tower heights merely allow to balance the eigenfrequencies between the frequency ranges of excitation—a so-called “soft-stiff” construction.

In case of steel tube towers this remains possible for turbines of capacity up to 2 MW. Thus the future multi-MW-turbines will need towers made of reinforced and pre-stressed concrete anyway, to reach the necessary stiffness. On the other hand concrete towers suffer from the problem of thermal constraints, which may influence the non-linear structural behaviour due to concrete cracking, and thus may also reduce the stiffness properties.

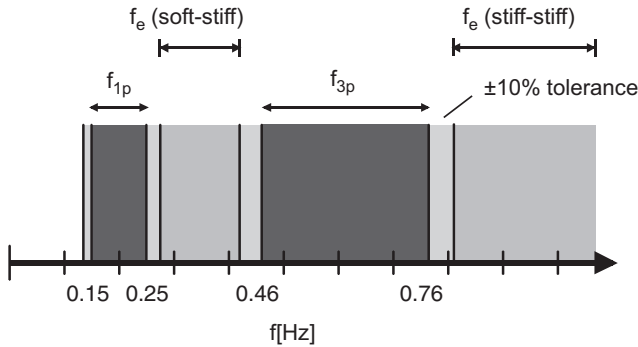


Fig. 4. Eigenfrequencies as design criteria for wind turbine towers.

So, the designer of a wind-turbine has to meet these thermal effects by an adequate numerical simulation to remain within the safe sector between the frequency ranges of excitation. Details of such simulations are given in Harte & Wörmann (2003) and in Wörmann (2004).

If this is considered, a quasi-static analysis of the structure remains valid. Simplified as a unit mass beam, the dynamic amplification factor  $\kappa$  for a periodic loading with frequency  $f_r$  reads as

$$\kappa = \left[ \left( 1 - \left( \frac{f_r}{f_e} \right)^2 \right)^2 + \left( \frac{\delta}{\pi} \cdot \frac{f_r}{f_e} \right)^2 \right]^{-1/2}, \tag{1}$$

with  $f_r$  is the frequency of excitation ( $f_{1p}$  or  $f_{3p}$ , respectively),  $f_e$  is eigenfrequency of the tower,  $\delta$  is logarithmic damping ratio.

#### 1.4. Fatigue

Classical fatigue accumulation rules according to Palmgren (1924) and Miner (1945) postulate a linear damage accumulation

$$D = \sum \frac{n_i}{N_i} \leq 1.0, \tag{2}$$

with  $n_i$  is the actual number of cycles,  $N_i$  is admissible number of cycles.

This linear assumption has proved to be sufficient for steel structures and is well established in the design of steel tube towers. On the other hand, wind energy turbines suffer much more from load-cycling than any other civil engineering structures. Due to the continuous rotation of the rotor numerous load-cycles will occur over life-time. In case of a turbine with a nominal rotor-blade frequency  $f_{3p} = 0.5$  Hz, we compute

$n = \pm 2 \cdot 10^6$	after 46 days under operation
$n = \pm 1 \cdot 10^8$	after 20 operating years with 2400 operating hours per year

Thus, the so-called cut-off limit is reached already in the first 2 or 3 months of the turbine life time. For steel, the residual fatigue strength is assumed to be unlimited beyond

this cutoff limit. This assumption has been proved by numerous experiments and by practical experience and thus is well established. For concrete any fundamental experience with high-cycle behaviour beyond 2 million cycles is still lacking. [CEB-FIP Model Code 90](#) provides the S-N-curves for concrete under compression, extrapolating experimental results from the low-cycle- to the high-cycle-range. The existence of a cutoff-limit for concrete is denied among experts.

In physical reality the assumption of linearity of damage accumulation can not be confirmed. The sequence of dynamic load intensity definitely influences the fatigue strength of structures, resulting in non-linear interactions between the number of load-cycles and the structural capacity. In the equation of motion the tangential stiffness matrix  $\mathbf{K}_T$  depends on the velocities  $\dot{\mathbf{V}}$  (viscous action), the deformations  $\mathbf{V}$  (elasto-plastic action) and especially the set of damage parameters  $\mathbf{d}$ . If we neglect damping effects in the state of equilibrium we can reduce the non-linear equation to an eigenvalue problem, but still considering pre-deformations and especially the damage effects  $\mathbf{d}$ .

$$\mathbf{M} \cdot \partial \ddot{\mathbf{V}} + \mathbf{K}_T(\mathbf{V}, \dot{\mathbf{V}}, \mathbf{d}) \partial \bar{\mathbf{V}} = 0, \quad (3)$$

where  $\mathbf{M}$  is the global mass matrix,  $\mathbf{K}_T$  is the tangential stiffness matrix,  $\mathbf{V}$ ,  $\dot{\mathbf{V}}$  is external nodal kinematic of the fundamental state,  $\partial \bar{\mathbf{V}}$ ,  $\partial \ddot{\mathbf{V}}$  are increments from the fundamental state to a neighbouring state,  $\mathbf{d}$  is a set of damage parameters.

This eigenvalue problem can be solved in selected load-steps during the complete incremental-iterative solution procedure. The resulting natural frequencies  $\omega_i$  may hold to define a global damage indicator  $D_i$

$$D_i = 1 - \frac{\omega_i(V, d)}{\omega_i(V, d = 0)} \quad (i = 1, m), \quad (4)$$

with  $D_i$  is the scalar damage indicators,  $D_i = 0$  is undamaged virgin state,  $D_i = 1$  is damaged-caused failure.

Herewith any state between virgin state and failure can be quantified, characterizing the loss of structural integrity over the structure's life-time.

Further results from simulations of cooling towers are given in [Noh et al. \(2003\)](#) and of wind turbine towers in [Harte & Wörmann \(2003\)](#) and [Wörmann \(2004\)](#). The combination of non-linear damage analyses with the classical damage accumulation rules in fatigue is still an issue open for research.

In the meanwhile the [CEB-FIP Model Code 90](#) offers a simplified method to consider the concrete fatigue resistance. As this method again is limited concerning the number of load-cycles, the new German guideline for wind energy turbines, [DIBt 2004](#), has extended the proof to  $2 \times 10^9$  load cycles:

$$S_{cd, \max} \leq 0.40 + 0.46 \cdot S_{cd, \min}, \quad (5)$$

where

$$S_{cd, \max} = \gamma_{sd} \cdot \sigma_{c, \max} / f_{cd, \text{fat}},$$

$$S_{cd, \min} = \gamma_{sd} \cdot \sigma_{c, \min} / f_{cd, \text{fat}},$$

with  $\gamma_{sd} = 1.1$  (partial safety factor for model inaccuracy),  $\sigma_{c, \max}$  is the absolute value of the max. compressive concrete stresses,  $\sigma_{c, \min}$  is absolute value of the min. compressive

concrete stresses at the same cross-section, where  $\sigma_{c,max}$  occurs ( $\sigma_{c,min} = 0$  in case of tensile stresses),  $f_{cd,fat}$  is design value of the fatigue strength of concrete under compression.

Eq. (5) is a conservative linearization considering the logarithmic S-N-curves.

1.5. Progressive damages and structural response

As a reference example, a prestressed concrete tower of a wind-turbine installed near Wilhelmshaven, Germany in 1992 will be analysed. It has a total height of 92 m and an installed capacity of 3 MW. It has been designed with respect to two wind load cases:

- extreme wind load (50 year periodic recurrence) in state “out-of-operation”,
- wind load at nominal power (= nominal wind velocity 14.15 m/s) with extreme gust and corresponding rotor loads in state “in-operation”.

Fig. 5 shows the overall dimensions of the tower and its meridional stress resultants  $n_{22}$ , considering

- dead-weight  $g$ ;
- meridional prestressing  $p$ ;
- wind load  $w$  from windward meridian  $0^\circ$ ;
- temperature load  $t$  consisting of
  - constant temperature  $\Delta T_N = 15\text{ K}$ , cosine-shaped due to solar radiation direction,
  - linear temperature gradient  $\Delta T_M = 15\text{ K}$ , along the total circumference.

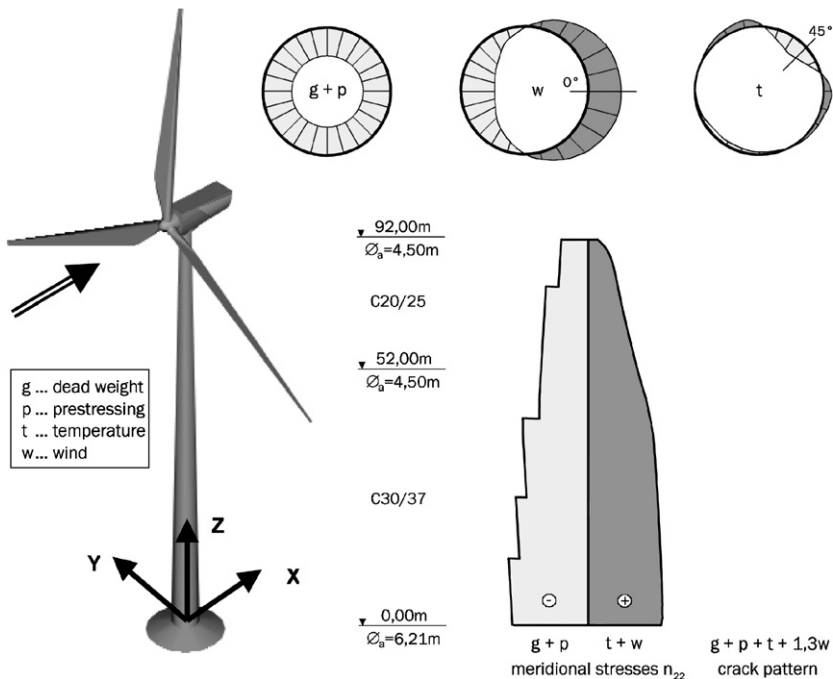


Fig. 5. Wind turbine tower with meridional stresses  $n_{22}$ .

It can be observed in Fig. 5 from the cross-sections of the meridional stresses that wind from 0° and solar radiation from 45° will yield tension in the tower shell, exceeding the compression by dead-weight and pre-stressing.

The non-linear ultimate-limit-state-analysis is performed by means of the finite-element-method, with the four-node isoparametric doubly curved shell element from (Basar et al., 1993) based on a Reissner-Mindlin-type shell theory. The material non-linearities of reinforcement and concrete are considered within a layered approach. It allows the accurate prediction of the stress distribution over the shell cross-section.

For simplification, the behaviour of concrete under compression has been assumed to remain linear. All other non-linear effects have been considered:

- tension cracking considering aggregate interlocking and kinematic crack closing mechanisms.
- tension stiffening concepts.
- elasto-plastic behaviour of the reinforcement steel.

The right side of Fig. 6 shows the non-linear load-displacement behaviour of the tower, namely the normal displacement at 0° at height 70 m. For the load case combination  $g+p+\lambda_3 \cdot w$ , a load factor of  $\lambda_3 = 1.60$  is achieved in the ultimate limit state.

In case the structure is stressed first by temperature loads  $\Delta T_N$  and  $\Delta T_M$ , the concrete tensile strength in circumferential direction will be exceeded already under  $\Delta T_M$ . This results in vertical bending cracks on the cold outer side of the tower. Because of the cosine-shaped, constant temperature part  $\Delta T_N = 15\text{ K}$ , meridional tensile stresses result at the intersection from warm to cold. In combination with tensile stresses due to wind, these stresses may initiate early cracking in the meridional direction, that means horizontal cracks across the concrete cross-section. The resulting reduction of bending strength and

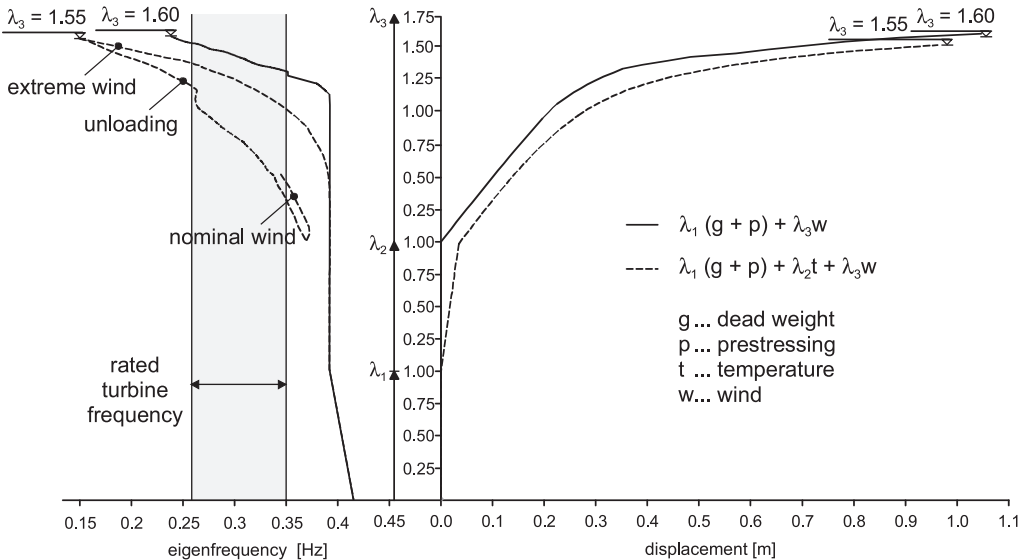


Fig. 6. Load-displacement-paths and eigenfrequencies of tower considering damage effects (displacement at windward meridian 0°, height 70 m).

stiffness yields higher deformations, and the decreased ability to redistribute stresses is characterized by a smaller load-carrying capacity  $\lambda_3 = 1.55$ .

The left side of Fig. 6 demonstrates the evolution of the first natural frequency  $\omega_1$ . In case of mere temperature loading we observe stiffness reduction in the load-displacement-graph, but there is no influence on the eigenfrequency. The reason is that only vertical cracks occur, which do not significantly influence the dynamic behaviour. In combination with wind load the thermal action will induce horizontal cracks at a lower wind load level, accompanied by a dramatic decrease of  $\omega_1$ , shown by the dotted line compared with the continuous line without thermal action.

The corresponding maximum damage in case of extreme wind load can be quantified by the eigenfrequency-based damage indicator acc. (4) to  $D_1 = 0.56$ , characterizing the residual distance to the critical state  $D_1 = 1.0$ . The results enable the estimation of the increase of the dynamic reaction, as in case of damage the decreasing eigenfrequency will shift the wind excitation towards its spectral peak. This can be shown by the standard von-Karman-spectrum, which clearly demonstrates the wind- and temperature-induced shift of the natural frequency from its virgin position towards the spectral peak and thus towards larger dynamic amplification of wind excitation. This will finally result in a progressive damaging process in case of multiple occurrence of extreme wind conditions.

Even if only one extreme storm has hit the structure, and the horizontal cracks have been closed by the prestressing—shown as the unloading path in Fig. 6—the resulting eigenfrequencies for wind-load-factor  $\lambda_3 = 0$  are closer to the dangerous range of the rated turbine excitation. So, if the turbine starts working again under nominal wind velocity 14.15 m/s, which approximately corresponds to a factor  $\lambda_3 = 0.5$  of extreme wind load, the eigenfrequency will be shifted into the rated frequency range and thus might be subjected to resonant dynamic excitations, heavily effecting the fatigue behaviour of the structure.

## 2. The innovative solar chimney concept

### 2.1. Idea

The Solar Chimney, illustrated schematically in Fig. 7, operates like a hydroelectric power plant, but instead of water, it uses hot air. This is particularly useful in arid areas, which are plentiful in Africa, even south of the Sahara.

It comprises a transparent roof collector, a central chimney tower and one or more turbo generators at the base. Beneath the collector, proposed to be a large, circular glass roof, air is heated. Through the coinciding change in air pressure, the air moves radially towards the centre, where it enters the tower, which creates an up-draught. By this suction effect, hot air is drawn in from the collector and as it rises up the chimney, it flows through either one large turbine, or numerous smaller turbines, the preferred option yet to be determined. These turbines are linked to conventional generators, whereby electricity is generated.

The output of the solar chimney is proportional to its size. The scale of a 1000–1500 m tall, 160 m diameter chimney tower, and a glass roof collector of diameter 4–7 km is proposed to produce an output of 200–400 MW. A study has recently been performed by Pretorius et al. (2004) to establish the total yearly output, considering day temperature cycle, cooler winter months, collector roof shape and height.

A 50 kW prototype solar chimney plant, with tower height 200 m and collector diameter 10 m, was built in Manzanares, Spain in 1982. Performance measurements on this

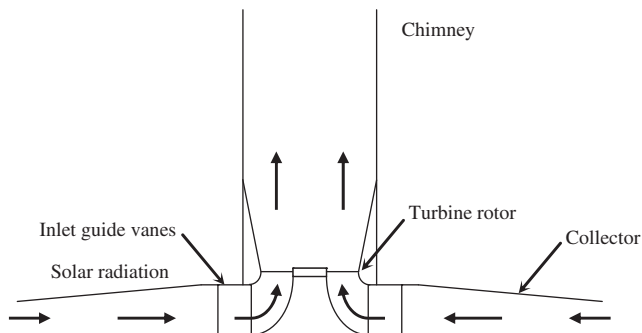


Fig. 7. Schematic representation of the solar chimney principle: glass roof collector, chimney tube and turbine.

experimental plant proved the solar tower concept to be technically reliable (Haaf et al. 1983, Haaf, 1984) and potentially economically viable (Schlaich, 1994). Since then, detailed studies of the performance of a solar chimney were performed and reported by Gannon and von Backström (2000), Kröger & Buys (2001) and Pretorius & Kröger (2006).

## 2.2. Wind profile

A true vertical wind profile for the entire height of the chimney is sought in order to determine the forces that will be exerted on the chimney structure. Until now, conservative extrapolated profiles have been used, as design profiles do not exist for altitudes above 500 m. Also, the wind-structural interaction must be studied to address potential aerodynamic instability of the tower.

For lack of wind measurement data above 300 m, several wind profiles have been proposed up to the tower height of 1500 m (Fig. 8). The most conservative wind profile, series 1, is obtained from the extrapolation of the wind speed at 10 m height

$$V_z = V_{10} k_r \left( \frac{z}{10} \right)^\alpha, \quad (6)$$

where  $V_z$  is the speed at height  $z$ ,  $V_{10}$  is the speed at 10 m height,  $k_r$  is a return period factor and  $\alpha$  is the terrain factor, varying from 0.16 for open terrain, to 0.21 in dense areas. For a wind speed of 40 m/s, a terrain factor of  $\alpha = 0.19$  and a 100 year return period factor of  $k_r = 1.04$  a wind speed of more than 100 m/s is computed from Eq. (6) at 1500 m height. A more favourable wind profile, series 2, is predicted by the formulation

$$V_z = V_{10} \ln \left( \frac{z}{z_0} \right) / \ln \left( \frac{z}{10} \right), \quad (7)$$

where,  $0.003 \leq z_0 \leq 0.10$  for open terrain,  $0.10 \leq z_0 \leq 0.20$  for outskirts of towns and cities by Simiu & Scanlan (1996), with  $z_0$  a terrain factor. For  $z_0 = 0.05$ , Eq. (7) computes a wind speed of 78 m/s at 1500 m. Envisaging solar chimney technology for South Africa, the South African loading code for buildings, SABS0160 (1989), is considered. This code prescribes the average wind velocities as shown by series 3 in Fig. 8 for a return period of

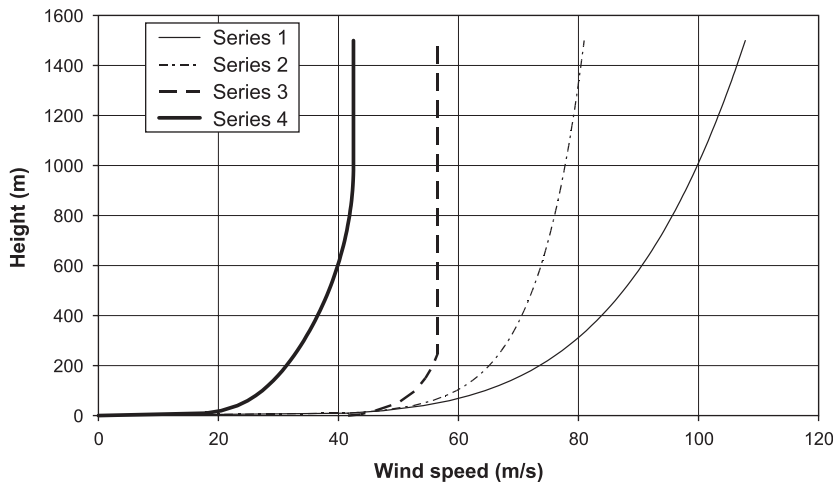


Fig. 8. Wind speed extrapolations to 1500 m height.

100 years, based on  $V_{10} = 40$  m/s. It suggests a gradient height of 250 m, where the maximum speed of  $V_{250} = 56$  m/s occurs, which remains constant beyond that height.

The existence of three air layers is acknowledged by the acceptance of the wind profile represented by series 4 in Fig. 8. In the lower region, roughly up to 200 m, friction dominates (Dyrbye and Hansen, 1997). In the upper region, beyond roughly 1000 m, the air flow becomes geostrophic, dominated by Coriolis forces (Dyrbye and Hansen, 1997), leading to a uniform wind velocity in this region. In the intermediate air layer, the so-called boundary layer, friction domination reduces gradually with height, as the Coriolis effect increases (Harris and Deaves, 1980). Wind measurement data from weather stations in the intended regions in South Africa suggest that a maximum 10 min average geostrophic wind speed of 42.5 m/s (Rousseau, 2005).

The investigation of vertical wind profiles of typhoons in Japan (Tamura, 2002) indicates the existence of such a gradient height, beyond which a near constant wind speed occurs up to heights of 3000 m.

### 2.3. Structural integrity

The size of the tower structure presents a challenge. It represents a leap beyond current building heights. If seismic regions are eliminated as potential sites for solar chimneys, wind remains the main action threatening structural stability, together with the immense weight. A reference set of dimensions of tower height 1500 m and internal diameter 160 m are used in subsequent discussions and result reporting. Also, the reference wall thickness variation with tower height shown in Fig. 9 is applicable.

It must be noted that the static, averaged wind speed profiles in Fig. 8 are fictitious, as real time wind measurements show large fluctuations, varying both spatially and in time. This leads to dynamic excitation of the structure by the wind, with the danger of resonance, potentially leading to collapse. Due to the random nature of wind, a frequency spectral analysis approach has been followed by Rousseau (2005) to study the structural response of the solar chimney. For this analysis, the series 4 wind speed profile was taken

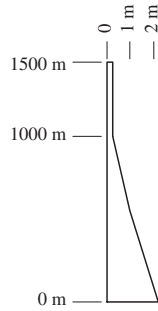


Fig. 9. Tower shell thickness (not to scale).

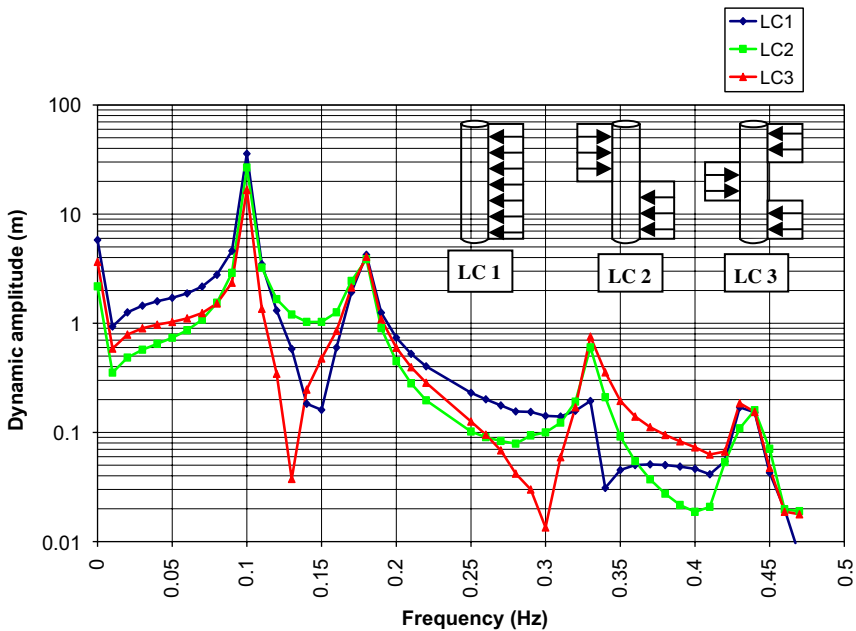


Fig. 10. Frequency response spectrum of tower top node.

as the mean wind speed, combined with a random gust described by a power spectral density function suggested by Davenport (1967). In lieu of characterized wind turbulence data beyond 200 m height, a gust amplitude of 6 m/s was considered reasonable. The structural response is shown in Fig. 10 as a frequency response spectrum, showing the maximum horizontal displacement of the top of the solar chimney as a function of the excitation frequency. Whereas the effect of the static wind profile (0 Hz) is a displacement of less than 10 m of the tower top, dynamic amplification occurs at the first natural frequency (0.1 Hz) of this structure, causing a top displacement of more than six times the static response. Note that modal damping of 1% of critical damping was considered in the analysis.

In addition to the uni-directional wind (LC1), the effect of wind inversions due to for instance thunderstorms (LC2 and LC3) was also studied. Note that the wind direction only

is indicated by the vectors in Fig. 10. The uni-directional wind dominates at low frequency, while the higher vibrational modes are excited by load cases 2 and 3. The large deformation under wind excitation at the low natural frequency of the solar chimney remains a concern.

Note that the particular case of spatially highly correlated wind velocity was considered in the above analyses. To obtain information about the structural response to generalized, spatially cross-correlated wind action, a stochastic dynamic analysis approach should be followed, which enables introduction of a load cross-correlation matrix. The results of such analyses will allow statistical treatment and derivation of structural response with particular levels of probability.

#### 2.4. Wind pressure

The static wind profile represented by series 4 in Fig. 8 is converted to pressures acting on the chimney along its height, as well as along the circumference. It is well known that wind pressure varies around the circumference of a tower. This pressure distribution is Reynolds number ( $R_e$ ) dependent, but also influenced by air flow axially (vertically) through the tower. By recent wind tunnel testing at  $9.3 \times 10^5 < R_e < 4.2 \times 10^6$  on a rigid model to scale 1:1000, the influence of the air flowing vertically through the tower, was simulated. The external pressures shown in Fig. 11 were measured for the case  $R_e = 4.2 \times 10^6$ , showing the influence of the air flowing vertically through the tower close to the top of the tower (at a distance 0.2 Diameter (0.2D) from the top) as well as lower down, at 1.2D from the top. The pressures stabilize at a distance roughly 0.65D from the top. The velocities of the vertical air flow through the tower were  $V_c = 0$  (no through flow) and  $V_c = 25$  m/s, respectively, and the model cross wind velocity  $V_a = 75$  m/s.

The internal pressure was also measured, as shown in Fig. 12 for the same through flow and external flow velocities as above. Only the measurements taken below 1D from the top are shown, confirming that also the internal pressures are stable in this region. The measurements confirm the SABS0160 (1989) suction coefficient of  $C_{pi} = -0.8$  for the case of no through flow. However, for a vertical air flow through the tower of 25 m/s the suction reduces to  $C_{pi} = -0.1$ . Note that the German VGB guideline (2005) prescribes  $C_{pi} = -0.5$  for cooling towers.

The pressure measurements provide the required information for static loading to the tower to establish structural integrity in terms of resistance to push over, as well as ovaling. In addition, points of separation of the boundary layer around the cylinder circumference may be identified. Thereby, some indication is given of potential uneven vortex shedding, which may cause aeroelastic instability of the tower. This is currently explored in more detail in further wind tunnel testing. Note, however, that the tower will experience air flow regimes beyond the critical Reynolds number at virtually any wind speed, due to its large diameter. This implies that optimal drag is achieved naturally, without the aid of increased roughness.

#### 2.5. Substructure design

A particular study was performed by Van Dyk and Van Zijl (2004) on a substructure concept for the solar chimney tower. The inlet guide vanes (IGV's), which direct air flow

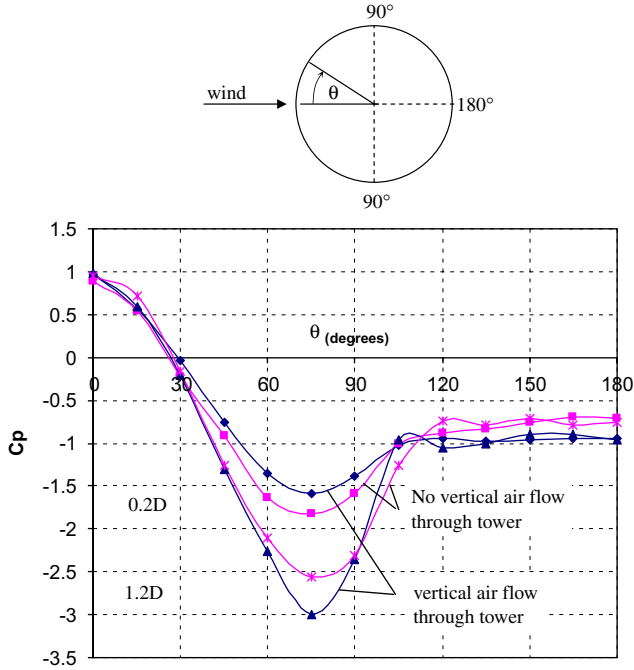


Fig. 11. External wind pressures at various positions along circumference.

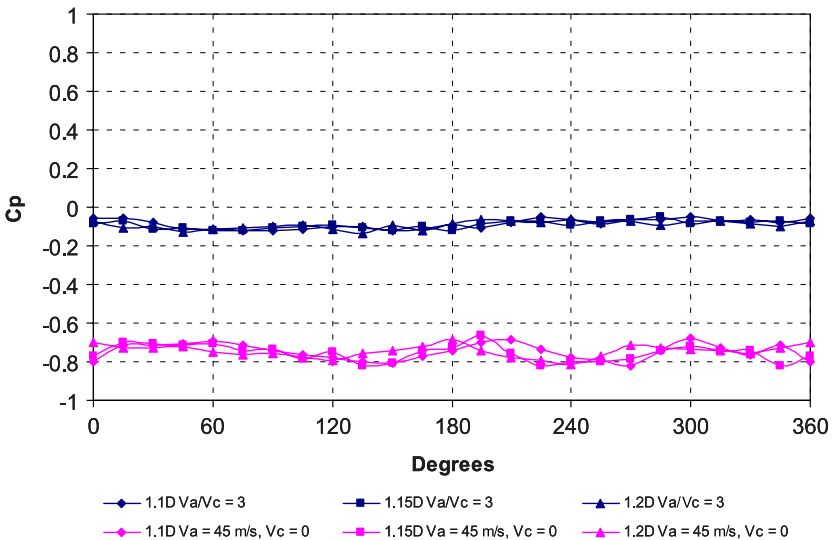


Fig. 12. Internal wind pressures at various positions along circumference.

from the collector into the turbine, in this case a single, central turbine as shown in Fig. 7, were used structurally for this purpose. Thereby, the IGV's transfer the own weight, but also the toppling, push-over effect of the wind to the foundations.

Gannon (2002) proposed the IGV layout shown in Fig. 13(a). 18 IGV's are aligned around the circumference, each rotated at  $10^\circ$  about the tower radius, to create pre-swirl of air onto the turbine blades. The IGV height is 60 m and the aerodynamic section 60 m in length, and 7.5 m wide at the widest part. To transmit the tower weight and wind lateral forces to the foundation, two alternative solutions shown in Fig. 13(b) and (c) were studied, both of reinforced concrete. The most conservative wind profile in Fig. 7 was considered. To relieve the large compressive stresses at the transition from tower shell to IGV, either the local enlargement in the shape of an anvil (Fig. 13(b)), or a system of combined bearing and shearing resistance of the fin stiffener (Fig. 13(c)) was required to limit the stress to within the capacity of contemporary medium-high strength concrete. Various sizes of anvils and fin stiffeners were considered in a cost optimization study, resulting in the cheapest option being a fin stiffener extending 40 m beyond the IGV height of 60 m. Note that the tower shell thickness variation with height shown in Fig. 9 was used.

Through eigenvalue analysis of the total tower, considering (i) a solid shell from the base to the top, (ii) the anvil type IGV support and (iii) the fin stiffener concept, the first global mode for each of these alternatives was computed to be within 5% of 0.1 Hz. This confirms that these choices of substructure do not influence the global stability significantly. However, the low base natural frequency remains a source of concern for this structure. To address this concern, alternative stiffening structures, as well as dampening systems are currently studied, while the wind characteristics at this altitude will be investigated to ascertain information about the excitation frequencies.

One of these alternative structures is shown in Fig. 14. To improve stiffness and dynamic stability of the chimney a twin-shell concept has been investigated by Sawka (2004). In the lower part a hyperbolic concrete shell has been added to

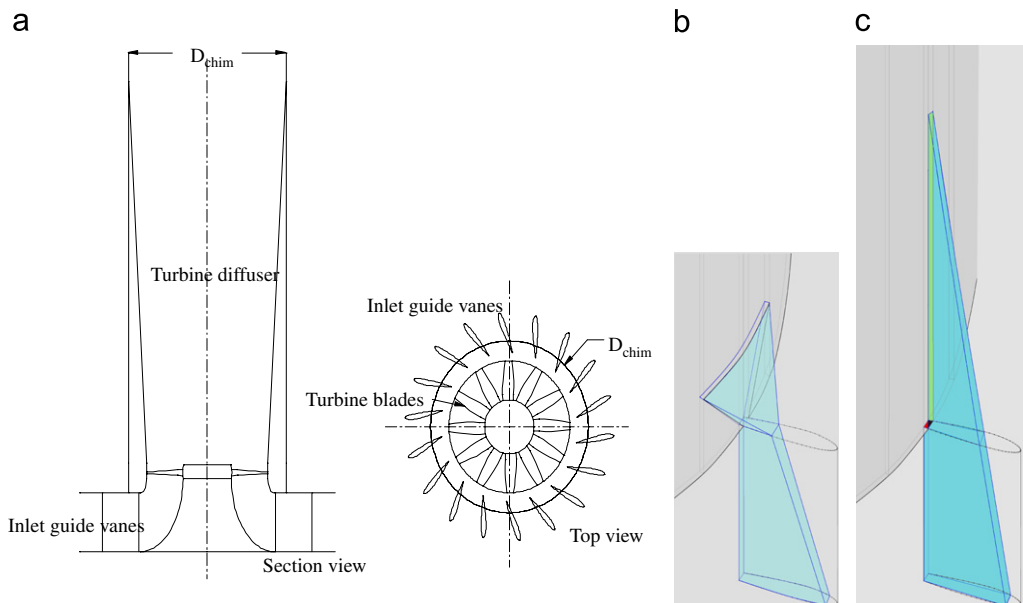


Fig. 13. (a) The layout of the eighteen IGV's (Gannon 2002). Alternative substructural systems (b), (c).

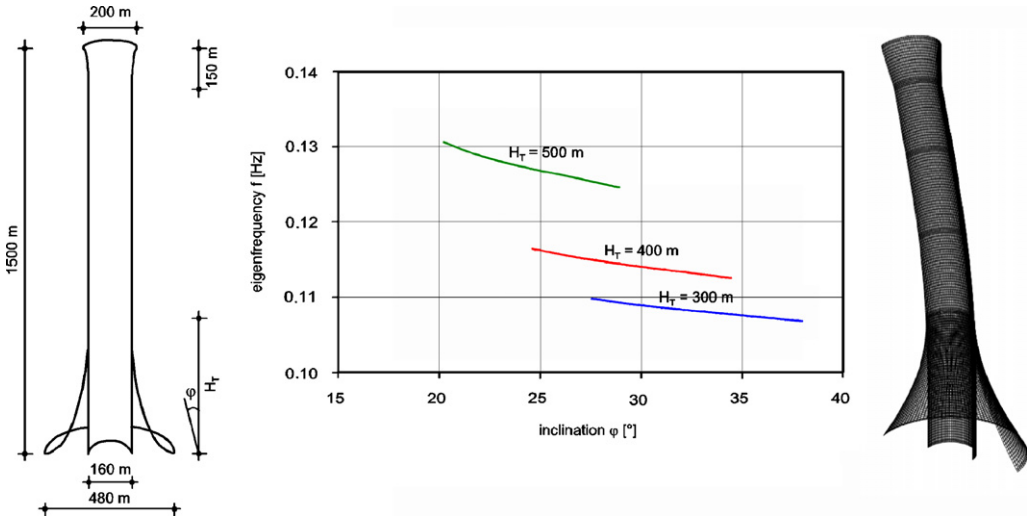


Fig. 14. Twin-shell concept: variation of parameters and eigenfrequencies.

the cylindrical shaft and as well at the top of the chimney the mouth has been opened by a hyperbolic shell as well. This structural alternative would fit best to a multiple horizontal-axis turbine concept.

By this concept both the horizontal deflections should be reduced and the eigenfrequencies should be enhanced in order to keep them away from the maximum of the wind spectral density. Thus, the structure could be improved more sufficiently against resonant excitations. Different heights  $H_T$  of the lower hyperbolic shell combined with different inclination angles  $\varphi$  have been investigated with respect to deflections, buckling loads, eigenfrequencies, and steel and concrete masses. For example, the variation of eigenfrequencies with respect to the varying geometric parameters and the first eigenmode are shown in Fig. 14.

### 3. Conclusions

The paper has presented some overall aspects of wind energy with special consideration on the dynamic excitation and fatigue behaviour. For future multi-MW-turbines concrete towers have been proved to be the adequate structural component. On the other hand, material non-linearities, like cracking and crushing of concrete, will heavily influence the dynamic behaviour and the long-term durability. The vice-versa dependence of damages and fatigue is still a matter of research in future.

Besides the expansion of classical wind turbines over the large-scale continent Africa, the innovative solar chimney concept may offer an additional alternative. In case of the existence of sufficient sunshine and space, together with an industrial demand for energy, the solar chimney could offer an alternative to classical fossil or nuclear power generation. These structures exceed the current engineering bounds. While insight into the wind action on the immense tower and its response have been developed and presented here, the concern of low natural frequencies remains. As for the increasingly

large wind turbines, the stiffness reduction, cracking and fatigue of the concrete structures remain research issues.

## Acknowledgements

The authors thank the German Research Foundation DFG and the Volkswagen Foundation for their support of parts of the presented research activities. Also, the authors gratefully acknowledge the support of students and colleagues at both universities in Stellenbosch and Wuppertal.

## References

- Basar, Y., Montag, U., Ding, Y., 1993. On an isoparametric finite element for composite laminates with finite rotations. *Comp. Mech.* 12, 329–348.
- CEB-FIP Model Code, 1990. CEB-FIB Model Code 1990 Design Code. Bulletin d'Information 195. Comité Euro-International du Béton, Lausanne.
- Davenport, A.G., 1967. Gust loading factors. *ASCE J. Struct. Division* 93, 11–34.
- DEWI, 2005. German Wind Energy Institute. *DEWI Magazin*, 27.
- DIBt, 2004. Guideline for wind energy turbines—action and static proof for tower and foundation, Ed. March 2004. Deutsches Institut für Bautechnik, Berlin.
- Dyrbye, C., Hansen, S., 1997. *Wind loads on structures*. Wiley, Chichester.
- Gannon, A.J., 2002. Solar chimney turbine performance. Dissertation presented for the Degree of Doctor of Philosophy at the University of Stellenbosch.
- Gannon, A.J., von Backström, T.W., 2000. Solar chimney cycle analysis with system loss and solar collector performance. *J. Solar Energy Eng.* 122, 133–137.
- Haaf, W., 1984. Solar chimneys, part II: Preliminary test results from the Manzanares pilot plant. *Int. J. Solar Energy* 2, 141–161.
- Haaf, W., Friedrich, K., Mayr, G., Schlaich, J., 1983. Solar chimneys, part I: Principle and construction of the pilot plant in Manzanares. *Int. J. Solar Energy* 2, 3–20.
- Harris, R.I. and Deaves, D.M., 1980. The structure of strong winds. The wind engineering in the eighties. In: *Proceedings of the Construction Industry, Research and Information Association (CIRIA) Conference*, London, pp. 4.1–4.93.
- Harte, R. & Wörmann, R., 2003. The Influence of Thermal Effects on the Load-bearing Behaviour of Concrete Wind-turbine Towers. In: *Proceedings of the 5th International Congress on Thermal Stresses and Related Topics, TS2003*, Blacksburg, USA, pp. WM-5-2-1-WM-5-2-4.
- Kröger, D.G. & Buys, J.D., 2001. Performance evaluation of a solar chimney power plant. *ISES 2001 Solar World Congress*, Adelaide, South Australia.
- Miner, M., 1945. Cumulative Damage in Fatigue. *J. Appl. Mech.* 12, 159–163.
- Noh, S.-Y., Meskouris, K., Harte, R., Krätzig, W., 2003. New design and damage assessment of large-scale cooling towers. *Struct. Eng. Mech.* 15 (1).
- Palmgren, A., 1924. Die Lebensdauer von Kugellagern. *VDI-Zeitschrift* 58, 339–345.
- Pretorius, J.P., Kröger, D.G., 2006. Critical evaluation of solar chimney power plant performance. *Solar Energy* 80 (5), 535–544.
- Pretorius, J.P., Kröger, D.G., Buys, J.D. & von Backström, T.W., 2004. Solar Tower Power Plant Performance Characteristics. *Fifth ISES Europe Solar Conference EuroSun2004*, Freiburg, pp. 1-870–1-879.
- Rousseau, J.-P., 2005. Dynamic evaluation of the solar chimney. MScEng-thesis, University of Stellenbosch, South Africa.
- SABS0160, 1989. South African Bureau of Standards 0160:1989. Loading Code.
- Sawka, M., 2004. Solar Chimney—Untersuchungen zur Strukturintegrität des Stahlbetonturms. *Bergische Universität Wuppertal*.
- Schlaich, J., 1994. *The Solar Chimney: Electricity from the Sun*. Deutsche Verlags-Anstalt, Stuttgart.
- Simiu, E., Scanlan, R.H., 1996. *Wind effects on structures*. John Wiley & Sons, New York.
- Tamura, Y., 2002. Recent Topics in Wind Engineering Focusing on Monitoring Techniques. *International Conference on Advances in Building Technology (ABT2002)*, Hong Kong.

- Van Dyk, C. & Van Zijl, G.P.A.G., 2004. Realisation of the inlet guide vanes—an integral part of the solar chimney. In: Proceedings of the Second International Conference on Structural Engineering, Mechanics and Computation, SEMC2004, Cape Town, South Africa, pp. 315–320.
- VGB Guideline, 2005. Structural Design of Cooling Towers. VGB PowerTech R 610 U.
- Wörmann, R., 2004. Analysis of the Progressive Damage Behaviour of Concrete Wind- Turbine Towers. In: Proceedings of the Second International Conference on Structural Engineering, Mechanics and Computation, SEMC2004, Cape Town, South Africa, pp. 303–307.